Jurnal Teknologi

Full Paper

EXPERIMENTAL AND FINITE ELEMENT ANALYSIS OF MODE I INTERLAMINAR FRACTURE ENERGY IN CARBON/EPOXY WOVEN LAMINATES

Muhammad Hadi Widanto*, Budi Aji Warsiyanto, Rini Wulandari

Department of Aeronautical Engineering, Universitas Dirgantara Marsekal Suryadarma, J Protokol Halim Perdana Kusuma Street, Komplek Bandara Halim Perdana Kusuma, Jakarta 13610, Indonesia

Article history
Received
14 November 2024
Received in revised form
1 June 2025
Accepted
1 June 2025
Published Online
27 February 2026

*Corresponding author
mhadi@unsurya.ac.id

Graphical abstract

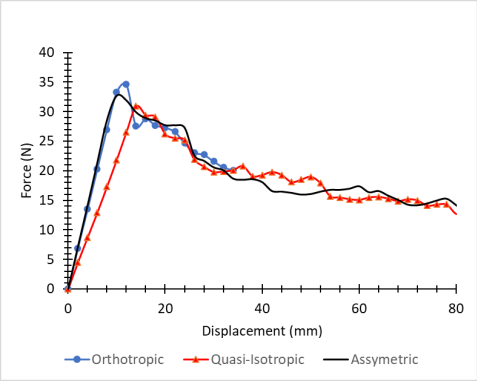

Abstract

Composite materials have been widely applied because they have advantages including high stiffness, strength and weight ratio. Composites also have the disadvantage of resistance to impact loads due to different damage modes compared to metallic materials. Delamination damage mode is the separation between layers causing a drastic decrease in properties to trigger catastrophic failure. One of the parameters to measure delamination resistance is fracture energy G_{IC} with the Double Cantilever Beam (DCB) test. This study aims to conduct experiments and simulations of DCB tests on twill weave woven carbon composite fibers made by Vacuum Assisted Resin Infusion (VARI) method. Quasi-isotropic, orthotropic and asymmetric fiber direction arrangements were tested to determine the effect of response and fracture energy values. Numerical modeling with Cohesive Zone Model (CZM) with 2D and 3D cohesive contact model provides an understanding of both models. The results show that the variation of stacking direction gives higher force response and lower fracture energy values. The higher bending stiffness leads to faster crack propagation. The orthotropic model provides higher stiffness so that the decrease in fracture energy value is quite significant. In the asymmetric model, the decrease in fracture energy due to the difference in stiffness of the adherent causes a slight decrease in the fracture energy value.

Keywords: Composite woven, double cantilever beam, Cohesive Zone Model, Vacuum Infusion, Fracture Energy

1.0 INTRODUCTION

Composites are widely applied in many industries because they offer several advantages, such as high strength and lightweight properties [1]. CFRP (Carbon Fiber Reinforced Polymer) is a type of composite material widely used in industry due to its excellent mechanical properties, namely high stiffness and strength [2]. The use of composite materials continues to grow in commercial jet aircraft and is gradually replacing conventional metals. This trend is expected to continue, contributing to a reduction in environmental exhaust emissions by 15%–20% in CO_2 emissions by the 2050 target [3] However, composite materials also have disadvantages, such as being sensitive to impact loads due to various damage modes [4]. Damage from impact loads on composites can result in delamination, leading to a reduction in residual strength and durability, and potentially causing catastrophic failure [5] .

Testing of composite materials regarding their mechanical properties, loading response, and

damage modes has been widely conducted, but most studies have focused on aerospace-grade composites manufactured using the prepreg method with an autoclave [6], [7]. Although this method provides high-quality specimens, it has limitations, including high production costs [8], [9]. Vacuum Assisted Resin Infusion (VARI) is a method that can reduce costs, where significant components are manufactured using vacuum bags instead of a rigid mold on the top side, while still utilizing a rigid mold at the bottom, yielding satisfactory manufacturing results [10], [11], [12]. This method can also be applied to other aircraft components, including floats for amphibious aircraft [13] Additionally, the advantages of woven fibers, which offer balanced strength in the plane directions when made with VARI, can provide good impact resistance [14].

Research on interlaminar properties is crucial in composites, particularly in assessing delamination resistance [15]. Delamination is a severe issue that can significantly reduce the structural strength and integrity, potentially leading to catastrophic failure [16], [17]. Fracture energy mode I (G_{IC}) is one of the key parameters for evaluating the development of delamination in composite laminates [16]. G_{IC} has a dominant effect on crack propagation leading to delamination damage [18]. Research on Double Cantilever Beam (DCB) tests with various parameter variations has been conducted to determine the effect on fracture energy values. DCB testing with the inclusion of nylon 6,6 nonwoven fabric has been shown to significantly increase fracture energy [19]. Studies on the effect of strain rate variation on DCB tests have also indicated a substantial influence. Additionally, DCB testing with variations in fiber interface types showed insignificant differences in fracture energy [20]. Research on DCB testing with variations in specimen width geometry has provided new perspectives on interfacial crack properties, particularly for studying delamination phenomena [21].

The Progressive Damage Model (PDM) is a simulation method that considers the initiation of damage, followed by the degradation of material stiffness [22]. There are three models commonly used to simulate delamination in composites: the failure criterion-based model, the fracture mechanics model, and the cohesive zone model. The failure criterion-based model calculates the interaction between out-of-plane compression and interlaminar shear stress, offering numerical efficiency, but the interface layers are not independent due to interactions between different failure modes [23]. The Virtual Crack Closure Technique (VCCT) is highly sensitive to mesh size, requiring higher computational performance and necessitating a pre-defined initial crack before simulation [24]. The Cohesive Zone Model (CZM) overcomes the limitations of VCCT by introducing initiation and propagation of damage with zero or quasi-zero thickness using a traction-separation law [25]. Numerical simulation with CZM can provide good correlation with DCB test results [26], [27]. Furthermore, the Peridynamic (PD) theory has also been developed to model Mode I delamination, demonstrating the force-displacement relationship and delamination migration in multidirectional composite laminates.

In this study, experiments and simulations of DCB tests manufactured using the VARI method are conducted. The objective is to investigate the effect of G_{IC} values under variations of quasi-isotropic, orthotropic, and asymmetric fiber stacking sequences. An in-depth understanding of how fiber orientations and stacking sequences influence crack propagation resistance is targeted. The CZM model is employed to evaluate the experimental results through numerical simulations. It is expected that analyzing both experimental and simulation results will provide deeper insight into the performance of composite materials for structural applications and contribute to the optimization and selection of suitable materials for damage-resistant applications.

2.0 METHODOLOGY

The materials tested were 2×2 twill weave carbon fiber HDC-522-3K, Bakelite epoxy resin EPR 174, and Bakelite hardener EPH 555 in a ratio of 1:1. The specimens were manufactured using the Vacuum Assisted Resin Infusion (VARI) method at room temperature with a curing time of 24 hours. An aluminium foil with a thickness of 15 µm was inserted at the mid-thickness of the laminate to form an initial crack in the specimen, as shown in Figure 1a. The setup for the resin impregnation process using the VARI method is shown in Figure 1b. During the impregnation process, negative pressure was applied to allow the resin to laminate the fibers with a uniform flow through the flow media, as shown in Figure 2.

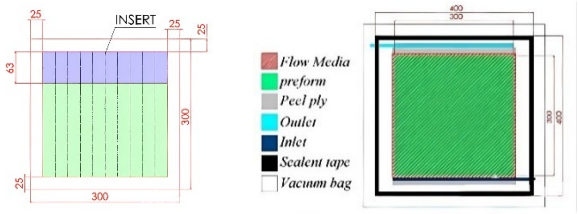

(a) (b)

Figure 1 set up Vacuum Infusion (a) inserted aluminium foil (b) set up overview

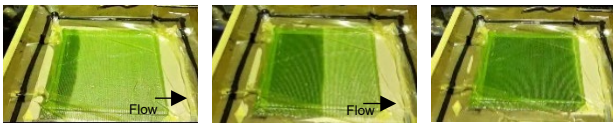

(a) (b) (c)

Figure 2 Impregnation Process (a) 25s (b) 50s (c) 148s

The resin flow rate at the inlet section decreased as the resin advanced toward the outlet section during the impregnation process. Once the entire preform was fully impregnated, a degassing process was conducted by allowing a few minutes for air evacuation after the inlet was closed. Degassing was carried out after the impregnation of the entire fiber was completed to reduce voids that might be trapped in the specimen [10].

Experimental tests were conducted in accordance with ASTM D5528 standards using a loading block [28]. The specimens were marked to determine crack growth during the test, as shown in Figure 3a. The tests were conducted at the Bandung Institute of Technology Materials Laboratory using an Instron 6800 (500 N load cell) with a loading rate of 5 mm/min, and the test setup is shown in Figure 3b. The fiber stacking sequences tested included quasi-isotropic, orthotropic, and asymmetric DCB responses. Details of the fiber stacking sequences for the three types of specimens are shown in Table 1. In the quasi-isotropic and orthotropic specimens, there are 12 plies, while in the asymmetric specimens there are 13 plies, with each layer having a thickness of 0.24 mm. The loading process, performed by pulling the loading block, caused crack propagation, as shown in Figure 3c. The fracture energy value can be calculated using the Modified Beam Theory (MBT) in Equation 1 and the Modified Compliance Calibration (MCC) method in Equation 2. P is the load, δ is the displacement, b is the specimen width, a is the delamination length, h is the thickness, A is the slope, and C is the root of compliance.

$$G_{IC(MBT)}=\frac{3P\delta}{2ba} \quad (1)$$

$$G_{IC(MCC)}=\frac{3P^2C^{2/3}}{2A_1bh} \quad (2)$$

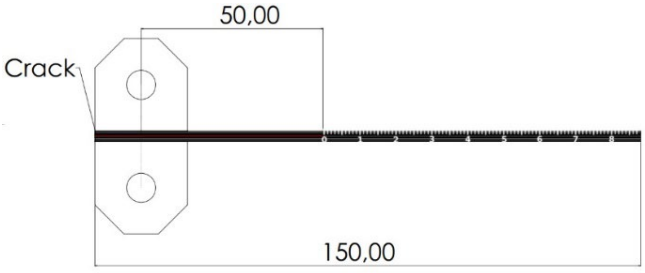

(a)

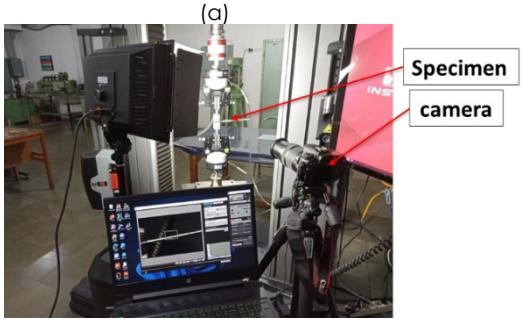

(b)

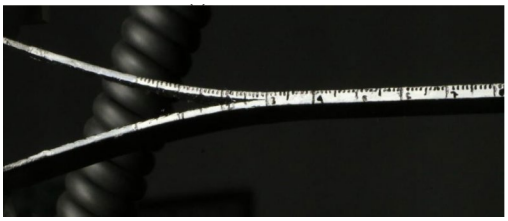

(c)

Figure 3 (a) DCB specimen (b) testing process (c) crack propagation during test

Tabel 1 Stacking direction

Quasi-Isotropic (12 plies)	[(0/90) / (+/-45) / (0/90) / (+/-45) / (0/90) / (+/-45) / inserted / (0/90) / (+/-45) / (0/90) / (+/-45) / (0/90) / (+/-45)]
Asymmetric (13 plies)	[(0/90) / (+/-45) / (0/90) / (+/-45) / (0/90) / (+/-45) / (0/90) / inserted / (+/-45) / (0/90) / (+/-45) / (0/90) / (+/-45) / (0/90)].
Orthotropic (12 plies)	$[(0/90)_6$ / inserted / $(0/90)_6]$

The Cohesive Zone Model (CZM) was used to simulate interlaminar damage and its propagation throughout the laminate. The constitutive equation for traction in the CZM is given in Equation 1. The CZM model does not require an initial crack to be predefined, and its main advantage lies in its ability to model damage initiation and propagation by defining a traction-separation law based on the strain energy release rate. It employs a bilinear traction-separation law for two surfaces: n (normal direction), and s and t (first and second in-plane shear), as shown in Figure 4. A layer of cohesive interaction was added at the mid-laminate of the FEM model using the bilinear traction-separation (t–δ) law, where t represents the cohesive interaction and δ represents the corresponding crack face opening displacement. The basic input properties are the cohesive fracture energy (Gc), cohesive strength (tn), and initial stiffness (k), which represent the area enclosed by the t–δ curve, the peak stress, and the initial slope, as defined in Equation 3.

$$t=\begin{bmatrix}t_n\\t_s\\t_t\end{bmatrix}=\begin{bmatrix}K_{nn} & K_{ns} & K_{nt}\\K_{ns} & K_{ss} & K_{st}\\K_{nt} & K_{st} & K_{tt}\end{bmatrix}\begin{Bmatrix}\delta_n\\\delta_s\\\delta_t\end{Bmatrix}=K\delta \quad (3)$$

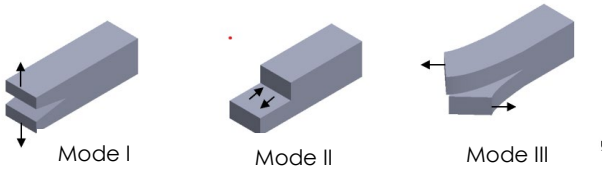

Figure 4 crack propagation mode I, mode II, mode III

The quadratic nominal stress (QUADS) and maximum nominal stress (MAXS) models are used to initiate damage in the traction-separation law, as described in Equation 4. QUADS is widely used because it provides good correlation with experimental results [29].]. Damage evolution occurs as softening takes place in the cohesive model. The damage variable, d, ranges from 0 to 1 and describes the degree of material property degradation. After damage initiation, the value of d is calculated based on Equation 3. δ_{eq}^{0} is initial damage initiation, δ_{eq} indicates the displacement when the critical value of damage initiation, sedangkan δ_{eq}^{f} is the displacement when total damage is experienced. δ_{eq} failure mode depends on the values of elastic stiffness and strength parameters specified at failure initiation. Each failure mode is specified with a fracture energy (G_{IC}) corresponding to the area of the triangle under the graph shown in Figure 5.

$$\text{MAXS} \qquad \left\{\frac{\langle t_n \rangle}{N_{max}}, \frac{t_s}{S_{max}}, \frac{t_t}{T_{max}}\right\} = 1 \tag{4}$$

$$\text{QUADS} \qquad \left(\frac{t_n}{N_{max}}\right)^2 + \left(\frac{t_s}{S_{max}}\right)^2 + \left(\frac{t_t}{T_{max}}\right)^2 = 1$$

$$d = \frac{\delta_{eq}^{f}(\delta_{eq} - \delta_{eq}^{0})}{\delta_{eq}(\delta_{eq}^{f} - \delta_{eq}^{0})} \tag{5}$$

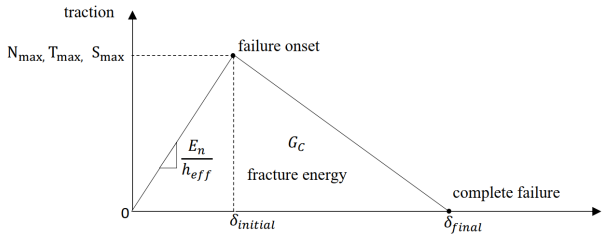

Figure 5 traction-separation curve of cohesive zone model

CZM implementation can be carried out in simulation models using two approaches: cohesive contact and cohesive elements. Both approaches are based on the same principle; however, the cohesive element model treats the cohesive region as an element with thickness, while cohesive contact defines it as an interface interaction. In addition, both 3D and 2D models were compared to assess the effects on computational time and the accuracy of correlation with experimental results. The model consists of 24,450 3D solid and shell continuum elements (SC8R). Boundary conditions were set such that the lower end of the sample was constrained in both translation and rotation (U1 = U2 = U3 = UR1 = UR2 = 0), while the upper end was subjected to a translational displacement in the y-direction (U2 = 100), corresponding to a displacement of 100 mm to promote crack propagation at the adhesive interface, as shown in Figure 6. Simulations were carried out under displacement control to closely match the experimental boundary conditions. The material properties of the carbon/epoxy composites are presented in Table 2.

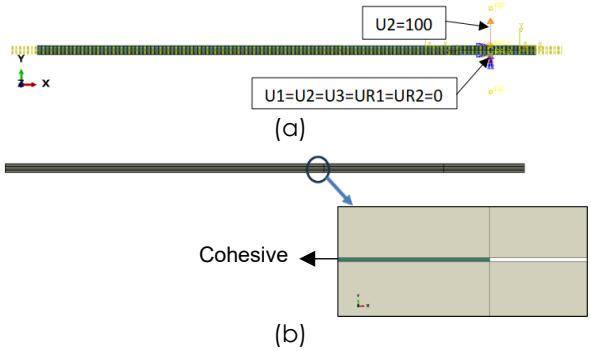

Figure 6 (a) Boundary Condition (b) Cohesive Zone Model

Tabel 2 Mechanical Properties carbon/epoxy

Parameter elastis					
E_1 (GPa)	E_2 (GPa)	ν_{12}	G_{12} (GPa)	G_{13} (GPa)	G_{23} (GPa)
52.3	52.3	0.006	2.7	1.35	1.35
Parameter cohesive contact					
N (MPa)	S (MPa)	T (MPa)	G_{IC} (N/mm)		
32	32	32	0.5		

N,S,T is cohesive strength normal and shear mode

3.0 RESULTS AND DISCUSSION

the double cantilever beam (DCB) test experiments with variations in stacking directions, such as quasi-isotropic, orthotropic, and asymmetric composite types, were conducted as shown in Figure 6. The experimental results for each sample variation were obtained using the MBT and MCC methods. The results obtained from the two methods are not significantly different; however, the variance among the specimens produced different outcomes, as shown in Table 3. The stacking variations show a significant and consistent decrease in the G_{IC} values across different calculation methods.

Table 3 G_{IC} for variance stacking type and different calculation methods

Stacking type	G_{IC} (N/mm) MBT	G_{IC} (N/mm) MCC
Quasi-isotropic	0.51	0.506
Asymmetric	0.45	0.42
Orthotropic	0.34	0.32

Figure 6 presents the results of the DCB test with G_{IC} calculations using the MBT method, which is more commonly applied. The results indicate that the

distribution of G_{IC} values for the quasi-isotropic stacking is broader compared to that of the asymmetric and orthotropic stackings. This suggests that the higher stiffness in the orthotropic laminate leads to greater crack growth, resulting in lower G_{IC} values, as shown in Figure 6. In the asymmetric stacking, the stiffness is slightly higher than in the quasi-isotropic stacking, which is reflected by the lower G_{IC} values compared to the quasi-isotropic stacking. These results demonstrate that the G_{IC} value is significantly influenced by the stacking direction of the composite due to variations in stiffness. Higher stiffness results in faster crack propagation during DCB testing. This can be observed during the softening process, where the force reduction relative to crack growth becomes steeper before reaching the plateau region. The fluctuations in the force–crack extension curve during the softening stage indicate the occurrence of fiber bridging during crack separation. Fiber bridging refers to the phenomenon where fiber stretch across and bridge the crack, helping to maintain the structural integrity of the laminate.

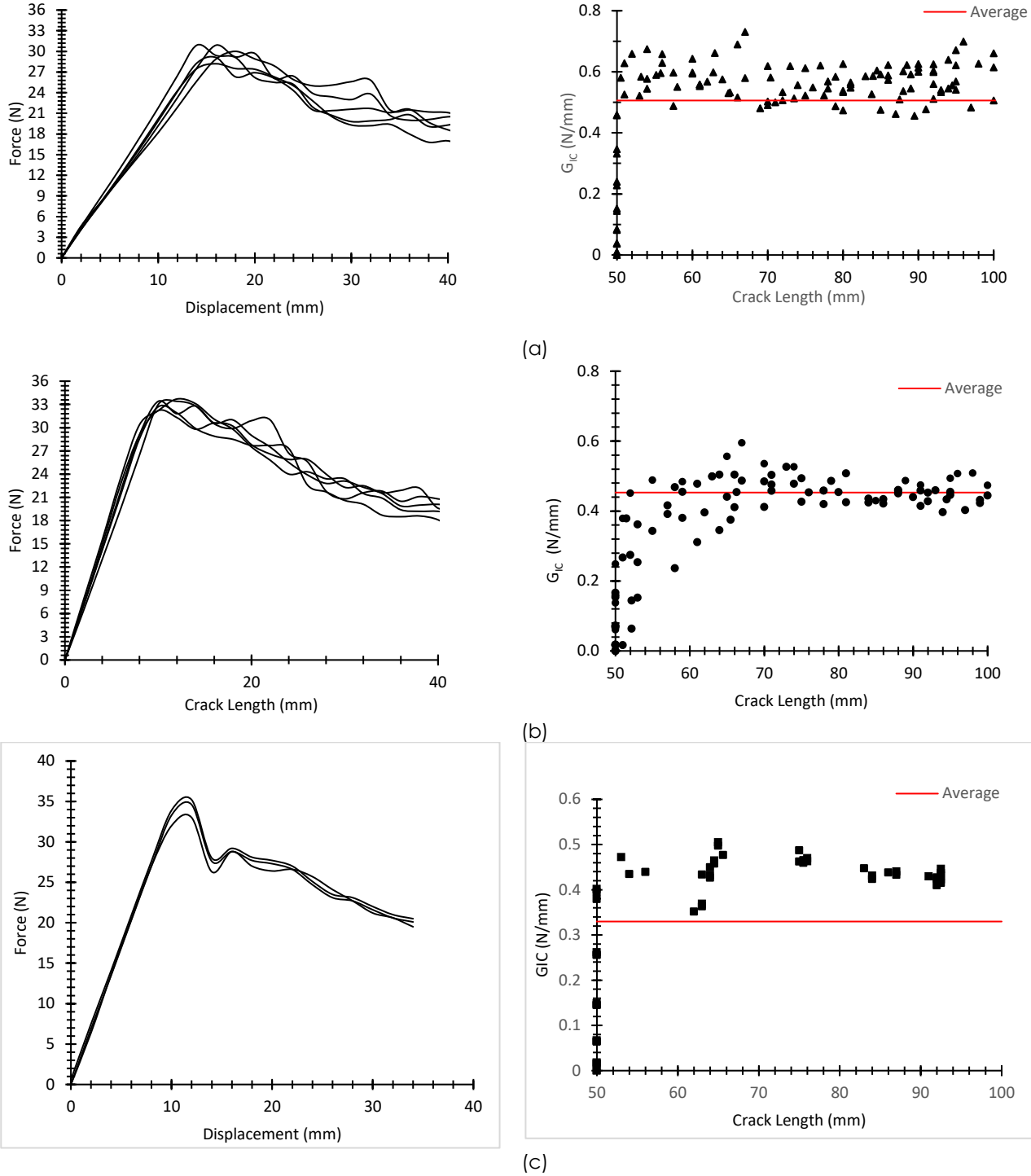

Figure 6 Experiment result (a) quasi-isotropic (b) asymmetric (c) orthotropic

The simulation model using CZM was evaluated on all three types of specimens. The CZM model was used with 2D and 3D modelling. The 2D test model has a better computational speed than the 3D model, but the response results differ slightly. The difference in element type affects the rotational displacement response due to the element response. In Figure 7 (a), the quasi-isotropic response graph gives similar results in 2D and 3D models, and the deviation is getting bigger in asymmetric and orthotropic. The results show that the 2D model causes a reduction in the accuracy of the stiffness response and softening process.

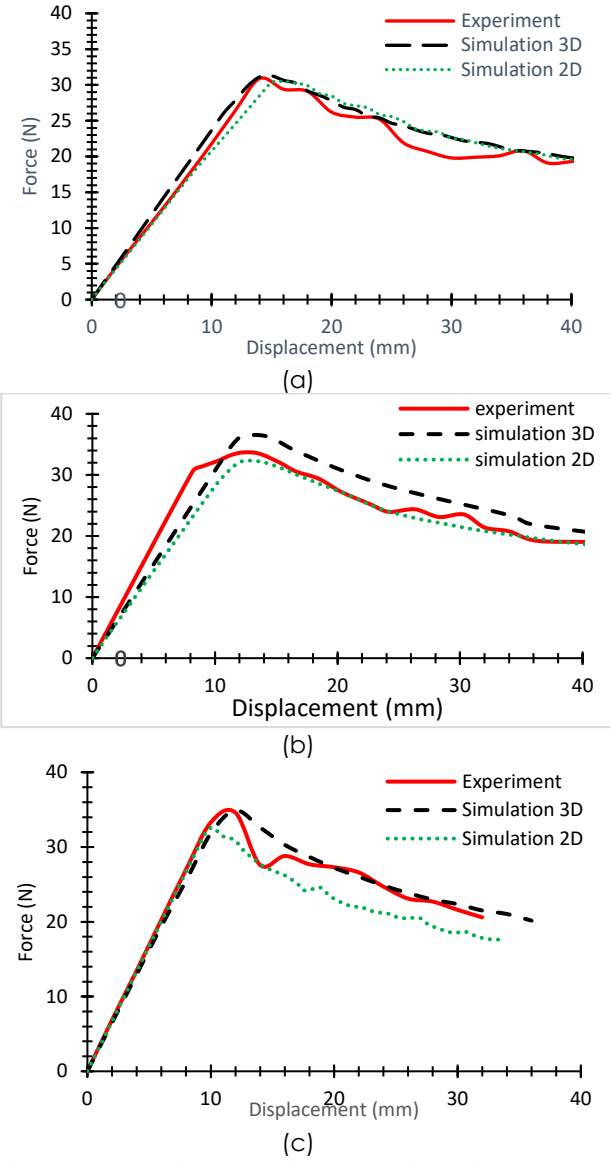

Figure 7 Comparison experiment and simulation 2D &3D (a) quasi-isotropic (b) asymmetric (c) orthotropic

In the comparison between simulation and experimental results, discrepancies were observed in the peak force and displacement responses during the softening phase. For the quasi-isotropic specimen, the simulation and experimental results demonstrated a relatively close agreement. Although minor deviations were identified during the softening process, both 3D and 2D simulations exhibited a strong correlation with the experimental data.

In the asymmetric model, the stiffness response in the experimental results was higher than that of the simulation, with differences in peak force between the 3D and 2D simulations amounting to 10.32% and 5.09%, respectively. During the softening phase, a similar correlation was observed, although there was a reduction deviation of 8.41% and 1.23%. For the orthotropic model, the peak force value obtained from the 3D simulation was relatively close to the experimental results, whereas the 2D model showed a discrepancy of 7.21%. In the softening phase, the average correlation between the experimental results and the 3D model was fairly good, while the 2D model exhibited an average deviation of 6.92%. Overall, the comparison between the experimental results and the simulation models using the CZM approach with various specimen configurations showed a good correlation. However, some discrepancies remain, mainly due to the simulation calculations being based on the G_{IC} value determined using the MBT method. Various methods for calculating the G_{IC} value have been developed to improve accuracy, thereby enhancing the overall precision of interlaminar modeling. [30], [31].

Fibre bridging is an important phenomenon that affects delamination strength in composite materials, especially during Delamination Cantilever Beam (DCB) testing. Factors such as the quality of the bond between the fibre and resin, the orientation and distribution of the fibre, and the thickness of the coating significantly affect the effectiveness of fibre bridging. Research shows that specimens with good bridging ability exhibit higher Mode I values, signifying better resistance to delamination. Figure 8 shows the fibre bridging that occurs in the quasi-isotropic specimen. The results show that apart from stiffness, fibre bridging due to variation in fibre direction can affect fracture energy.

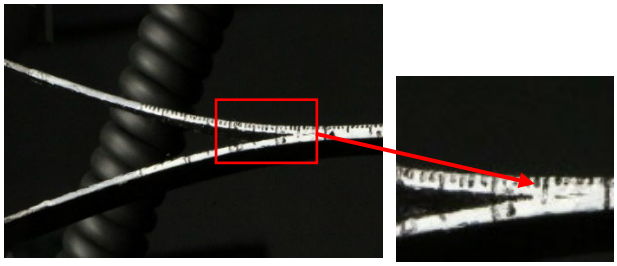

Figure 8 Fiber bridging

4.0 CONCLUSION

The stacking direction variation in DCB specimens results in different force responses and fracture energy values. Increased specimen rigidity leads to a more significant peak force response, with the maximum

force observed in the orthotropic, asymmetric, and quasi-isotropic specimens, respectively. This rigidity also causes a reduction in fracture energy values. The more rigid the specimen, the longer the crack propagation relative to a given displacement load. The simulation results using the CZM method and a cohesive contact model show good correlation with the experimental results. In both the 2D and 3D models, the resulting force responses are not significantly different; however, the 3D model provides a slightly better response than the 2D model due to a more accurate representation of stiffness. Furthermore, the results indicate that variations in fiber direction lead to fiber bridging, which can significantly influence the fracture energy values.

Acknowledgement

The authors gratefully acknowledge Universitas Dirgantara Marsekal Suryadarma and Institut Teknologi Bandung for their approved funding and laboratory support, which enabled this important research to be conducted effectively. We also extend our gratitude to the Directorate of Research and Community Service, Ministry of Research, Technology, and Higher Education for providing scientific article writing training.

Conflicts of Interest

The authors declare that there is no conflict of interest regarding the publication of this paper.

References

[1] McIlhagger, A., E. Archer, and R. McIlhagger. 2019. Manufacturing Processes for Composite Materials and Components for Aerospace Applications. *Polymer Composites in the Aerospace Industry*. 59–81. Elsevier. https://doi.org/10.1016/B978-0-08-102679-3.00003-4.

[2] Chen, A. Y., S. Baehr, A. Turner, Z. Zhang, and G. X. Gu. 2021. Carbon-Fiber Reinforced Polymer Composites: A Comparison of Manufacturing Methods on Mechanical Properties. *International Journal of Lightweight Materials and Manufacture*. 4(4): 468–479. https://doi.org/10.1016/j.ijlmm.2021.04.001.

[3] Bachmann, J., C. Hidalgo, and S. Bricout. 2017. Environmental Analysis of Innovative Sustainable Composites with Potential Use in Aviation Sector—A Life Cycle Assessment Review. *Science China Technological Sciences*. 60(9): 1301–1317. https://doi.org/10.1007/s11431-016-9094-y.

[4] Al Omari, A. S., K. S. Al-Athel, A. F. M. Arif, and F. A. Al-Sulaiman. 2020. Experimental and Computational Analysis of Low-Velocity Impact on Carbon-, Glass- and Mixed-Fiber Composite Plates. *Journal of Composites Science*. 4(4): 148. https://doi.org/10.3390/jcs4040148.

[5] Wisnom, M. R. 2012. The Role of Delamination in Failure of Fibre-Reinforced Composites. *Philosophical Transactions of the Royal Society A: Mathematical, Physical and Engineering Sciences*. 370(1965): 1850–1870. https://doi.org/10.1098/rsta.2011.0441.

[6] Liao, B., *et al.* 2020. Effect of Double Impact Positions on the Low Velocity Impact Behaviors and Damage Interference Mechanism for Composite Laminates. *Composites Part A: Applied Science and Manufacturing*. 136: 105964. https://doi.org/10.1016/j.compositesa.2020.105964.

[7] Sasikumar, A., D. Trias, J. Costa, N. Blanco, J. Orr, and P. Linde. 2019. Effect of Ply Thickness and Ply Level Hybridization on the Compression after Impact Strength of Thin Laminates. *Composites Part A: Applied Science and Manufacturing*. 121: 232–243. https://doi.org/10.1016/j.compositesa.2019.03.022.

[8] Shaik, F., M. Ramakrishna, and P. D. Varma. 2021. A Review on Fabrication of Thermoset Prepreg Composites Using Out-of-Autoclave Technology. *INCAS Bulletin*. 13(2). https://doi.org/10.13111/2066-8201.2021.13.2.13.

[9] Bere, P., E. Sabău, C. Dudescu, C. Neamtu, and M. Fărtan. 2019. Experimental Research Regarding Carbon Fiber/Epoxy Material Manufactured by Autoclave Process. *MATEC Web of Conferences*. 299: 06005. https://doi.org/10.1051/matecconf/201929906005.

[10] Juan, J., A. Silva, J. A. Tornero, J. Gámez, and N. Salán. 2021. Void Content Minimization in Vacuum Infusion (VI) via Effective Degassing. *Polymers*. 13(17): 2876. https://doi.org/10.3390/polym13172876.

[11] Saputra, A. H., and G. Setyarso. 2016. Vacuum Infusion Equipment Design and the Influence of Reinforcement Layers Addition to the Resin Infusion Time. *IOP Conference Series: Materials Science and Engineering*. 162: 012015. https://doi.org/10.1088/1757-899X/162/1/012015.

[12] Park, C. H., and A. Saouab. 2009. Analytical Modeling of Composite Molding by Resin Infusion with Flexible Tooling: VARI and RFI Processes. *Journal of Composite Materials*. 43(18): 1877–1900. https://doi.org/10.1177/0021998309341848.

[13] Lailatul Muzayadah, N., *et al.* 2022. Investigation of the Mechanical Properties of Vinyl Ester Carbon Composites through Immersion in Seawater and Freshwater Using the VARI (Vacuum Assisted Resin Infusion) Method. *Indonesian Journal of Aerospace*. 20(1): 9–24. https://doi.org/10.30536/j.jtd.2022.v20.a3579

[14] Ge, X., P. Zhang, F. Zhao, M. Liu, J. Liu, and Y. Cheng. 2022. Experimental and Numerical Investigations on the Dynamic Response of Woven Carbon Fiber Reinforced Thick Composite Laminates under Low-Velocity Impact. *Composite Structures*. 279: 114792. https://doi.org/10.1016/j.compstruct.2021.114792.

[15] Dai, G., L. Zhan, B. Ma, C. Guan, and M. Huang. 2023. Effect of Process Parameters on Interlaminar Properties of Thermoplastic Composite: Molecular Dynamics Simulation and Experimental Verification. *Polymer*. 280: 126062. https://doi.org/10.1016/j.polymer.2023.126062.

[16] Huang, T., and M. Bobyr. 2023. A Review of Delamination Damage of Composite Materials. *Journal of Composites Science*. 7(11): 468. https://doi.org/10.3390/jcs7110468.

[17] Wang, K., L. Zhao, H. Hong, J. Zhang, and Y. Gong. 2021. Parameter Studies and Evaluation Principles of Delamination Damage in Laminated Composites. *Chinese Journal of Aeronautics*. 34(7): 62–72. https://doi.org/10.1016/j.cja.2020.10.022.

[18] Vieille, B., V. M. Casado, and C. Bouvet. 2014. Influence of Matrix Toughness and Ductility on the Compression-after-Impact Behavior of Woven-Ply Thermoplastic- and Thermosetting-Composites: A Comparative Study. *Composite Structures*. 110: 207–218. https://doi.org/10.1016/j.compstruct.2013.12.008.

[19] Beylergil, B., M. Tanoğlu, and E. Aktaş. 2020. Experimental and Statistical Analysis of Carbon Fiber/Epoxy Composites Interleaved with Nylon 6,6 Nonwoven Fabric Interlayers. *Journal of Composite Materials*. 54(27): 4173–4184. https://doi.org/10.1177/0021998320927740.

[20] Rzeczkowski, J., S. Samborski, and M. de Moura. 2020. Experimental Investigation of Delamination in Composite Continuous Fiber-Reinforced Plastic Laminates with Elastic

Couplings. *Materials.* 13(22): 5146. https://doi.org/10.3390/ma13225146.
[21] Budzik, M. K., S. Heide-Jørgensen, and R. Aghababaei. 2021. Fracture Mechanics Analysis of Delamination along Width-Varying Interfaces. *Composites Part B: Engineering.* 215: 108793. https://doi.org/10.1016/j.compositesb.2021.108793.
[22] Zhou, J., P. Wen, and S. Wang. 2019. Finite Element Analysis of a Modified Progressive Damage Model for Composite Laminates under Low-Velocity Impact. *Composite Structures.* 225: 111113. https://doi.org/10.1016/j.compstruct.2019.111113.
[23] Hou, J. P., N. Petrinic, and C. Ruiz. 2001. A Delamination Criterion for Laminated Composites under Low-Velocity Impact. *Composites Science and Technology.* 61(14): 2069–2074. https://doi.org/10.1016/S0266-3538(01)00128-2.
[24] Krueger, R. 2004. Virtual Crack Closure Technique: History, Approach, and Applications. *Applied Mechanics Reviews.* 57 (1–6): 109–143. https://doi.org/10.1115/1.1595677.
[25] Camanho, P. P., C. G. Dávila, and M. F. De Moura. 2003. Numerical Simulation of Mixed-Mode Progressive Delamination in Composite Materials. *Journal of Composite Materials.* 37(16): 1415–1438. https://doi.org/10.1177/0021998303034505.
[26] Škec, L., G. Alfano, and G. Jelenić. 2019. Complete Analytical Solutions for Double Cantilever Beam Specimens with Bi-Linear Quasi-Brittle and Brittle Interfaces. *International Journal of Fracture.* 215(1–2): 1–37. https://doi.org/10.1007/s10704-018-0324-5.
[27] Park, S.-Y., and H.-Y. Jeong. 2022. Determination of Cohesive Zone Model Parameters for Tape Delamination Based on Tests and Finite Element Simulations. *Journal of Mechanical Science and Technology.* 36(11): 5657–5666. https://doi.org/10.1007/s12206-022-1028-3.
[28] ASTM International. 2013. *ASTM D5528-13: Standard Test Method for Mode I Interlaminar Fracture Toughness of Unidirectional Fiber-Reinforced Polymer Matrix Composites*. West Conshohocken, PA: ASTM International. https://doi.org/10.1520/D5528-13.
[29] Patel, A., E. Sato, N. Shichijo, I. Hirata, and T. Takagi. 2022. A Mixed XFEM and CZM Approach for Predicting Progressive Failure in Advanced SiC/SiC CMC Component. *Composites Part C: Open Access.* 9: 100325. https://doi.org/10.1016/j.jcomc.2022.100325.
[30] Wang, Z., Y. Gong, Z. Ding, L. Yan, Y. Zhang, and N. Hu. 2024. A New Method for Determining Fracture Toughness and Bridging Law of Asymmetric Double Cantilever Beam. *Engineering Fracture Mechanics.* 309: 110428. https://doi.org/10.1016/j.engfracmech.2024.110428.
[31] Medina, S. A., E. V. González, N. Blanco, J. Pernas-Sánchez, and J. A. Artero-Guerrero. 2023. Guided Double Cantilever Beam Test Method for Intermediate and High Loading Rates in Composites. *International Journal of Solids and Structures.* 264: 112118. https://doi.org/10.1016/j.ijsolstr.2023.112118.